Talanta 116 (2013) 122–126

Contents lists available at ScienceDirect

Talanta

journal homepage: www.elsevier.com/locate/talanta

Neural networks to estimate the water content of imidazolium-based ionic liquids using their refractive indices

José S. Torrecilla*, César Tortuero, John C. Cancilla, Pablo Díaz-Rodríguez

Department of Chemical Engineering, Complutense University of Madrid, E-28040 Madrid, Spain.

ARTICLE INFO

Article history:
Received 22 January 2013
Received in revised form
13 April 2013
Accepted 21 April 2013
Available online 6 May 2013

Keywords:
Ionic liquid
Refractive index
Water content
Relative humidity

ABSTRACT

A non-linear model has been developed to estimate the water content of 1-butyl-3-methylimidazolium tetrafluoroborate, 1-butyl-3-methylimidazolium methylsulfate, and 1,3-dimethylimidazolium methylsulfate ionic liquids using their respective refractive index values. The experimental values measured to design the neural network (NN) model were registered at 298.15 K. These were determined at different relative humidity values which ranged from 11.1% to 84.3%. The estimated results were compared with experimental measurements of water content obtained by the Karl Fischer technique, and the differences between the real and estimated values were less than 0.06% in the internal validation process. In addition, an external validation test was developed using bibliographical references. In this case, the mean prediction error was less than 5.4%. In light of these results, the NN model shows an acceptable goodness of fit, sufficient robustness, and a more than adequate predictive capacity to estimate the water content of the ILs through the analysis of their refractive index.

1. Introduction

Ionic liquids (ILs) are salts which remain in liquid state below or near 100 °C. They are formed by organic and inorganic ions that result in a huge number of possible ILs with unique properties [1,2]. Due to the great number of existing ILs and their exceptional properties, they are essential compounds in different fields such as organic synthesis, bio-catalysis, nanotechnology, extraction processes, and others [3,2]. Therefore, they are currently being vastly employed in many applications from the scientific and industrial fields all around the world [4,5].

Although molten salts were discovered over 200 years ago, the most relevant research projects related with these compounds started in the last quarter of the XX century and have continued until today [6]. Therefore, the current known facts about their properties are still limited. To overcome this lack of information, research groups are publishing their findings (physicochemical properties, new applications, models, and more) in scientific journals, international conferences, or databases.

Due to the fact that the value of various physicochemical properties of ILs (viscosity, density, surface tension, refractive index, *etc.*) highly depends on their purity, the bibliographical information must be handled accordingly [7–10]. Therefore, it is important to develop a suitable method which easily detects the impurities in ILs, such as water content or halides, by taking advantage of accessible and common properties. Because of the already commented lack of information on this topic, Torrecilla et al. have recently developed some tools for the estimation of the water content in imidazolium ILs. The measurement of their thermodynamic properties was combined with mathematical models based on lineal algorithms, chaotic parameters and neural network (NN) models [9,11]. As a continuation of that work, and in an attempt to simplify this technique, the refractive index (RI) has been studied. The reason behind the choice of this physicochemical property is that it is not only sensitive to impurities (water content), but also very easy to measure [1]. It is therefore a good candidate to be used in order to achieve the aforementioned objective.

In particular, the goal of this work is to create a simple NN model capable of estimating the property-affecting water content present in 1-butyl-3-methylimidazolium tetrafluoroborate (bmim[BF_4]), 1-butyl-3-methylimidazolium methylsulfate (bmim[$MeSO_4$]), and 1,3-dimethylimidazolium methylsulfate (mmim[$MeSO_4$]) ILs by the measurement of their refractive index values.

2. Materials and methods

In addition to the databases and neural network used, all of necessary equipment and chemicals to measure the refractive indices and the water content of the aforementioned ILs are presented in this section. These three properties have been modified changing the relative humidity of air in a range of 11.1–84.3% at 298.15 K using salt solutions (*vide infra*).

* Corresponding author. Tel.: +34 91 394 42 44; fax: +34 91 394 42 43.
E-mail addresses: jstorre@ucm.es, jstorre@quim.ucm.es (J.S. Torrecilla).

0039-9140/$ - see front matter © 2013 Elsevier B.V. All rights reserved.
http://dx.doi.org/10.1016/j.talanta.2013.04.047

Table 1
Purity, water, and halides mass fractions of the chemicals used.

Chemical	Purity mass fraction	Water mass fraction	Halides mass fraction	Supplier
bmim[BF_4]	≥0.99	2.48×10^{-4}	$< 1 \times 10^{-4}$	IoLiTec
mmim[$MeSO_4$]	≥0.99	1.84×10^{-5}	$< 1 \times 10^{-4}$	
bmim[$MeSO_4$]	≥0.99	6.81×10^{-5}	$< 1 \times 10^{-4}$	
Lithium chloride	≥0.99			Panreac chimie S.A.R.L.
Potassium acetate	≥0.99			
Magnesium chloride 6-hydrate	≥0.99			
Potassium carbonate	≥0.99			
Sodium dichromate 2-hydrate	≥0.995			
Sodium bromide	≥0.99			
Sodium nitrite	≥0.98			
Potassium chloride	≥0.9995			

Table 2
Relative humidities (RHs) of saturated salt solutions at 298.15 K in the equilibrium [14].

Chemical	RH(%)
Lithium chloride	11.1
Potassium acetate	22.5
Magnesium chloride	32.5
Potassium carbonate	43.7
Sodium dichromate	53.3
Sodium bromide	58.1
Sodium nitrite	64.4
Potassium chloride	84.3

Table 3
Comparison of measured pure bmim[BF_4], bmim[$MeSO_4$], and mmim[$MeSO_4$] ILs (exp.) with literature values (lit.) at 298.15 K.

Ionic liquid	RI	
	exp.	**lit.**
bmim[BF_4]	1.4218	1.4218[a]
mmim[$MeSO_4$]	1.4799	1.4827[b]
bmim[$MeSO_4$]	1.4797	1.47942[c]

[a] Ref. [15].
[c] Ref. [16].
[b] Ref. [17].

2.1. Reagents, solutions and instrumentation

2.1.1. Chemicals

Details of suppliers, water content, halides mass fraction, and purity of every compound used in this work can be found in Table 1. The aqueous solutions were prepared using ultra-pure water obtained from a Milli-Q water purification system (Millipore, Saint Quentis Yvelines, France).

All the IL samples used were dried by heating at 333 K for 24 h under reduced pressure. All experiments were carried out in a vacuum atmosphere glove box under dry nitrogen due to the sensitivity of the ILs to air moisture. Every sample was prepared in triplicate, and then, each one was analyzed three times. The water content of the sample was measured before and after each property determination [8,12]. The non-IL compounds shown in Table 1 are used to create eight different relative humidity environments inside the hydration equipment described below.

2.1.2. Hydration equipment

In order to determine the absorption equilibrium moisture of bmim[BF_4], bmim[$MeSO_4$], and mmim[$MeSO_4$] an isopiestic method was used [13,14]. The equipment and the experimental procedure have already been described in detail by Torrecilla et al. [9]. For every IL utilized, several runs were carried out in an atmosphere with different air moisture values that were generated by saturated solutions of various salts in water at 298 K and atmospheric pressure. The relative humidities (RHs) in the equilibrium of the eight saturated salt solutions at 298.15 K are listed in Table 2. Every IL was hydrated until the relative change of the water content rate, WCR (described by Eq. (1)), between two consecutive mass measurements of the container was ≤0.03% h^{-1}.

$$\mathrm{WCR} = \frac{Ms(t+1) - Ms(t)}{tMso} 100 \quad (1)$$

where *Mso*, *Ms*, and *t* are the initial sample mass, the sample mass, and the hydration time in hours, respectively. In this way, eight different solutions of water in the three ILs were made utilizing the saturated salt solutions listed in Table 2. When the water absorption equilibrium was reached, the refractive indices of the ILs were measured (*vide infra*).

2.1.3. Refractive index

Refractive indices (RIs) of the binary mixtures composed of bmim[BF_4], bmim[$MeSO_4$], or mmim[$MeSO_4$] and water at 298.15 K and under atmospheric pressure were determined using a J357 Automatic Refractometer (Rudolph Research Analytical). The standard uncertainty in these experimental measurements has been found to be less than $\pm 9 \times 10^{-5}$. As it can be seen in Table 3, there is a satisfactory correlation between the RI values for pure ILs presented here and the values published in literature [15,16,17].

2.1.4. Water content

Water content determination of the aqueous solutions of bmim[BF_4], bmim[$MeSO_4$], and mmim[$MeSO_4$] ILs was carried out utilizing a Karl Fischer titrator DL31 from Mettler Toledo and using the one-component technique. For volumetric Karl Fischer titration, dry methanol (CH_3OH, Riedel-de Haën, HYDRANAL-water mass fraction $< 0.01\%$) and standard Riedel-de Haën (HYDRANAL-standard (5.00 ± 0.02) mg mL^{-1} as water) were used. The polarizing current for the potentiometric end-point determination was 20 A and the stop voltage 100 mV. The end-point criterion was the drift stabilization (3 μg H_2O min^{-1}) or maximum titration time (10 min). The measurement was corrected for the baseline drift, defined as the residual or penetrating water that the apparatus removes per minute. The uncertainty of the water content measurements was estimated to be less than ± 2.5%.

2.2. Neural network model

The neural network applied is a multilayer perceptron which is formed by several artificial neurons arranged in two layers (topology of the NN): hidden and output layers, where the non-linear

calculations are done. In addition to this, there is an input layer constituted by nodes, which are used to enter data into the NN.

The calculation process in each neuron involves both activation and transfer functions. The calculation of the activation function, Eq. (1), is the sum of the multiplied input data inserted into each neuron by a self-adjustable parameter w, called weight; the result, x_k, is fed into a transfer function. The most used training algorithms are the sigmoid, hyperbolical tangent, and linear transfer functions (TFs), Eqs. (2), (3), and (4), respectively. The calculated value, y_k, is the output that results from the calculations which take place in a neuron.

$$x_k = \sum_{j=1} w_{jk} y_j \tag{1}$$

$$y_k = f(x_k) = \left(\frac{1}{1+e^{-x_k}}\right) \tag{2}$$

$$y_k = f(x_k) = \left(\frac{1-e^{-2x_k}}{1+e^{-2x_k}}\right) \tag{3}$$

$$y_k = f(x_k) = x_k \tag{4}$$

The learning process, which updates the weights to improve the estimative capacity of the NN, is carried out by minimizing the combination of the squared errors and the variation of the weights to be optimized by the Bayesian regulation backpropagation (trainBR) as the training function [18]. This function uses the *Jacobian* for calculations, which assumes that the performance is a mean or sum of squared errors [19]. Using this method, the correct combination of weights is achieved, and consequently, the optimized NN is able to generalize well. TrainBR is a network training function that updates the weight and bias values according to Levenberg–Marquardt optimization [19]. One of the most important features of the training function used here is that it provides a measure of how many network parameters (weights and biases) are being effectively used by the network [19]. Since only the most important parameters of the NN are optimized, the number of data points required for the optimization process is reduced. Because of that, in the NN presented here, the over-fitting effect is avoided and generalization capability is favored.

Apart from the weights, the NN has other parameters such as topology, Marquard adjustment parameter (learning coefficient, Lc), decrease factor for Lc (Lcd), or increase factor for Lc (Lci) [20]. Detailed information about these NN parameters can be found in the work of Demuth et al. [19]. The neural network used was designed with Matlab version 7.01.24704 (R14) [19].

2.3. Learning and verification database

Following the aforementioned protocols, the three ILs studied were partially hydrated, and then, their water content was measured. The databases used to optimize the neural network model applied have been created from the measurements of refractive index and water content of every ionic liquid (*vide supra*), and four datasets taken from literature. As an example, the RI of the ILs used here *versus* the relative humidity of air is shown in Fig. 1.

The general database is formed by 94 datasets, Table 4. Every sample is constituted by one independent variable (RI) and one dependent variable (water content) for a given IL. The database was divided randomly into three groups: learning, verification, and validation samples. The learning sample is used to optimize the model, and the verification and validation databases are only used to evaluate its performance. The learning and verification datasets contain 80 and 10% of the general database, respectively. The two validation sets contain the remaining 10%, Table 4. Taking into account that the verification and validation sample ranges must be within the learning sample range, every dataset of the global database was randomly distributed into the verification and internal validation samples. In addition, to check the generalization capacity of the NN model, an external validation has been done. To develop it, experimental data available in the literature was employed [21-24]. All of the accessed referenced data offers similar information. Table 4 presents the number of samples used in each learning, verification, and validation processes.

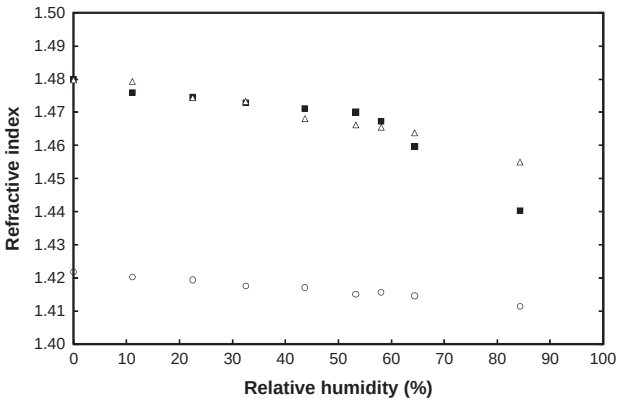

Fig. 1. Refractive indices of the ionic liquids at 298.15 K as a function of the relative humidity of the air (○, bmim[BF_4]; ■, mmim[$MeSO_4$]; ▲, bmim[$MeSO_4$]).

Table 4
Number of samples used in the learning, verification, and the two validation processes.

Ionic liquid	Number of samples				Total
	Learning	Verification	Internal validation	External validation	
bmim[BF_4]	25	3	2	1[a]	**31**
bmim[$MeSO_4$]	25	3	2	2[b]	**32**
mmim[$MeSO_4$]	25	3	2	1[c]	**31**
Total	**75**	**9**	**6**	**4**	**94**

[a] Ref. [21].
[b] Refs. [22 and 23].
[c] Ref. [24].

The applicability domain of the data used in the learning, verification, and two validation samples has been evaluated following the calculation process described in literature [25,26], which consists of determining the compounds with cross-validated standardized residuals greater than three standard deviation values. No anomalous data set was found.

3. Results and discussion

The optimization, verification, and validation processes of the NN model applied to estimate the water content (dependent variable) of bmim[BF_4], bmim[$MeSO_4$], and mmim[$MeSO_4$] ILs using their RI values as independent variables are described in this section.

3.1. Neural network model optimization

In the design of the NN model, its parameters (topology, Lc, Lcd, and Lci) were optimized. The NN used is formed by three layers (input, hidden, and output), a topology widely used to analyze several problems [20]. There is a single node in the input layer to introduce the RI values, and one output neuron to offer the estimation of the ILs water content. The hidden neuron number

(HNN) and other parameters of the NN has been fixed by optimization techniques (*vide infra*).

Regarding the training function, the Bayesian regulation back-propagation algorithm was selected because its generalization power is higher than other training functions, and avoids the over-fitting when a small learning sample is used [19]. To prevent the NN from over-fitting, the learning process was repeated while the verification Mean Square Error, MSE, defined by Eq. (5), decreased, and continued until this error started to rise. A detailed description of the calculation process is described in literature [27].

$$\mathrm{MSE} = \frac{1}{N}\sum_{k=1}^{N}(r_k - y_k)^2 \quad (5)$$

In Eq. (5), N, y_k, and r_k are, respectively, the number of samples of the database, the response of the output neuron, and the corresponding real output values. The HNN and NN parameters are optimized in a single step using a statistical experimental design based on the Box-Wilson Central Composite Design 2^4+Star Points. The experimental factors analyzed were Lc and Lcd (between 1 and 0.001) and Lci (between 2 and 100) [27]. Considering the learning sample size, the HNN range selected was between 2 and 8 neurons [28]. The responses of the statistical experimental design were the mean prediction error (MPE), Eq. (6), and the adjusted correlation coefficient (R_a^2). Because the main goal is to have a NN that estimates results with the highest accuracy possible, the defined requirements of the statistical experimental design were to obtain the least mean prediction error with the highest values of R_a^2 possible. Both indices are easily computed and provide a good description of the predictive performance of the network [29].

$$\mathrm{MPE} = \frac{1}{N}\sum_{k=1}^{N}|r_k - y_k| \quad (6)$$

After considering that the water content of three ILs should be estimated with the lowest performance error possible, a HNN equal to 3 was selected. The optimized parameters of the NN models are shown in Table 5. It is very troublesome to establish a relation between the optimal parameters and each system. It is important to understand that the main goal of the optimization of a NN model is not to find the best possible option, but to find a model which best fulfills the user's requirements.

These obtained statistical results of the NN model are accurate enough to allow testing its applicability on real cases. Therefore, this optimized NN model has been internally and externally validated with data from different sources (*vide infra*).

3.2. Application of the NN model

During the entire validation process, the optimized NN model is not updated, that is, all NN parameters (weights, HNN, Lc, Lcd, and Lci) are maintained fixed. In order to carry out the validation of the optimized model, the previously mentioned internal validation sample was employed, Fig. 2. The mathematical procedure followed was similar to the verification process described above. Therefore, to calculate the water content (dependent variable) of the ILs, the refractive indices (independent variable), which were never used before, from the internal validation are inputted into the optimized NN model. The statistical results of the estimated *versus* the experimental values ($R_a^2 > 0.99$ and MPE $< 0.06\%$) are close to those calculated in the verification process. This is mainly because the internal validation and the other two databases (learning and verification samples) have been created under similar experimental conditions (*vide supra*).

Table 5
Parameters of the neural network model and statistical results in the verification process (estimated *versus* experimental values).

Parameter	Optimized value
Transfer function	Sigmoid
Training function	TrainBR
Hidden neuron number	3
Lc	0.01
Lcd	0.001
Lci	10
Final prediction error	
MPE (%)	< 0.05
R_a^2	> 0.99

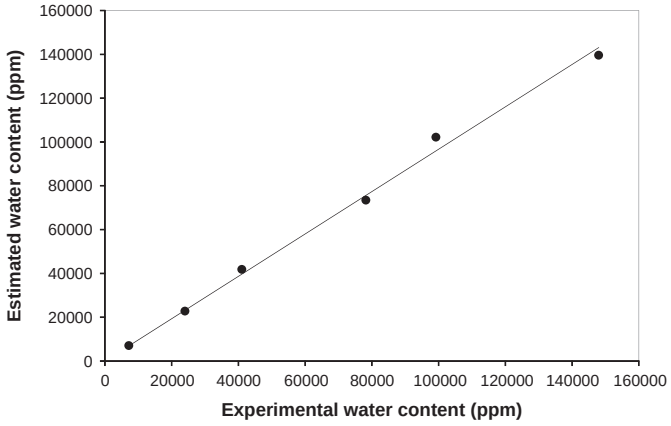

Fig. 2. Experimental *versus* estimated water content values calculated using the internal validation sample.

The optimized NN model has been externally validated with other experimental values from different sources (scientific references). In this stage, the generalization capacity of the model will be evaluated using four scientific references with information about the water content and its respective RI values of the three ILs were studied here [21–24] (*vide supra*). The independent variables have been input into the optimized NN model, and then the water content values of the ILs have been estimated. The adjusted correlation coefficient and MPE are higher than 0.91 and less than 5.4%, respectively. As it can be expected, these results are worse than the internal validation and verification processes mainly because the syntheses of the ILs, the existing impurities, and the analytical equipment employed were different. Nevertheless, considering that the sources of the data used came from a variety of references with their own experimental conditions, the statistical results are more than adequate and therefore, these statistical results verify that this NN model is adequate to estimate the water content of these ILs. Similarly, these statistical results confirm that the user can detect the studied impurity as a previous step to the use of information from literature. These statistical results are similar to the aforementioned estimations obtained from a NN based on thermodynamic properties [11].

Taking into account the statistical results of the verification and validation processes, the optimized NN model has sufficient robustness and predictive capacity to estimate the water content of these three ionic liquids studying their refractive index in the working range of the relative humidity used (11.1–84.3% at 298.15 K). To sum up, the water content (in the range studied) can be estimated by the NN model presented here.

4. Conclusions

The water content values of 1-butyl-3-methylimidazolium tetrafluoroborate, 1-butyl-3-methylimidazolium methylsulfate, and 1,3-dimethylimidazolium methylsulfate ILs have been estimated using

their refractive indices values by a neural network multilayer perceptron model. The water content and, therefore, the refractive index of the ILs have been modified by changing the relative humidity of the air in a range of 11.1–84.3% at 298.15 K. The RIs of the ILs were measured when the water absorption equilibrium was reached.

Once the NN model was designed and optimized, it was analyzed and tested using three methods *viz*. verification, internal validation, and external validation processes. During the verification and internal validation processes, the water content was estimated with a MPE of less than 0.05 and 0.06%, respectively. In addition, in order to check the generalization capability of the optimized NN model, it has been tested using external databases from scientific references. In these cases, although the statistical results are obviously worse (MPE $<5.4\%$), the generalization of the NN model is fulfilled.

To sum up, taking the statistical results into account, this NN model shows an acceptable goodness of fit, sufficient robustness, and an adequate predictive capacity to estimate the water content of the ionic liquids studied by their refractive index. Therefore, this technique is not only valid to estimate the purity of ILs, but also is adequate to easily predict their water content. Consequently, in the range tested, the neural network multilayer perceptron model created is an interesting tool for an on-line control of the water content present in the ILs employed by simply measuring their RI.

Acknowledgments

The research leading to these results has achieved funding from the European Union Seventh Framework Programme (FP7/2007–2013) under Grant Agreement no. HEALTH-F4-2011-258868.

References

[1] P. Wasserscheid, T. Welton, Ionic Liquids in Synthesis, Second edition, Wiley-VCH, Weinheim, 2008.
[2] J.S. Torrecilla, The Role of Ionic Liquids in the Chemical Industry, Nova Science Publishers, Inc., New York, 2012.
[3] N.V. Plechkova, K.R. Seddon, Chem. Soc. Rev. 37 (2008) 123–150.
[4] R.D. Rogers, K.R. Seddon, Science 302 (2003) 792–793.
[5] M. Freemantle, Chem. Eng. News 76 (1998) 32–37.
[6] M. Gaune-Escard, K.R. Seddon, Molten Salts and Ionic Liquids, John Willey & Sons Inc., USA, 2010.
[7] K.R. Seddon, A. Stark, M.J. Torres, Pure Appl. Chem. 72 (2000) 2275–2287.
[8] J.A. Widegren, A. Laesecke, J.W. Magee, Chem. Commun. (2005) 1610–1612.
[9] J.S. Torrecilla, T. Rafione, J. García, F. Rodríguez, J. Chem. Eng. Data 53 (2008) 923–928.
[10] H.F.D. Almeida, J.A. Lopes-da-Silva, M.G. Freire, J.A.P. Coutinho, J. Chem. Thermodyn. 57 (2013) 372–379.
[11] J.S. Torrecilla, E. Rojo, J.C. Domínguez, F. Rodríguez, Talanta 81 (2010) 1766–1771.
[12] H. Rodríguez, J.F. Brennecke, J. Chem. Eng. Data 51 (2006) 2145–2155.
[13] W.A. Wink, Ind. Eng. Chem. Anal. Ed. 18 (1946) 251–252.
[14] J.S. Torrecilla, J.M. Aragón, M.C. Palancar, Eur. J. Lipid Sci. Technol. 108 (2006) 913–924.
[15] A. Soriano, B. Doma, M. Li, J. Chem. Thermodyn. 41 (2009) 301–307.
[16] A.B. Pereiro, P. Verdia, E. Tojo, A. Rodriguez, J. Chem. Eng. Data 52 (2007) 377–380.
[17] A.B. Pereiro, J.L. Legido, A. Rodriguez, J. Chem. Thermodyn. 37 (2008) 1168–1175.
[18] J.S. Torrecilla, J.M. Aragón, M.C. Palancar, Ind. Eng. Chem. Res. 47 (2008) 7072–7080.
[19] H. Demuth, M. Beale, M. Hagan, Neural Network Toolbox for Use with MATLAB® User's Guide. Version 4.0.6. Ninth printing Revised for Version 4.0.6 (Release 14SP3), Natick, Massachusetts, 2005.
[20] J.S. Torrecilla, J.M. Aragon, M.C. Palancar, Ind. Eng. Chem. Res. 44 (2005) 8057.
[21] I.B. Malham, M. Turmine, J. Chem. Thermodyn. 40 (2008) 718–723.
[22] A.B. Pereiro, A. Rodríguez, J. Chem. Thermodyn. 39 (2007) 978–989.
[23] T. Singh, A. Kumar, J. Solution Chem. 38 (2009) 1043–1053.
[24] E. Gómez, B. González, N. Calvar, Á. Domínguez., J. Chem. Thermodyn. 40 (2008) 1208–1216.
[25] P. Gramatica, QSAR Comb. Sci. 26 (2007) 694–701.
[26] P. Gramatica, E. Giani, E.J. Papa, J. Mol. Graph. Model. 25 (2007) 755–766.
[27] J.S. Torrecilla, A. Fernández, J. García, F. Rodríguez, Ind. Eng. Chem. Res. 46 (2007) 3787–3793.
[28] Y. Sun, Y. Peng, Y. Chen, A.J. Shukla, Adv. Drug Deliver. Rev. 55 (2003) 1201–1215.
[29] L.B. Sheiner, S. Beal, J. Pharmacokinet. Biopharm. 9 (1981) 503–512.